

# Computer Controlled IR Spectrometer Using a Color Center Laser

G. LITFIN, C. R. POLLOCK, J. V. V. KASPER, R. F. CURL, JR., AND FRANK K. TITTEL, SENIOR MEMBER, IEEE

**Abstract**—A high resolution IR spectrometer for the 2.2–3.3  $\mu\text{m}$  range has been developed using a computer controlled CW color center laser. Computer control makes possible single-frequency scans of up to 100  $\text{cm}^{-1}$  with a resolution determined by the cavity mode spacing (250 MHz) and continuous high resolution scans (linewidth below 1 MHz) over 1  $\text{cm}^{-1}$  ranges. The laser spectrometer has been tested on the NO overtone band at 2.68  $\mu\text{m}$ .

## INTRODUCTION

THE recent development of single-mode color center lasers with wavelengths as large as 3.33  $\mu\text{m}$  opens new possibilities for investigation of molecular species in the near IR. Of special interest is high sensitivity, high resolution spectroscopy of X-H stretch fundamentals ( $X = \text{F}, \text{O}, \text{N}, \text{C}$ ). The color center laser (CCL) has all the desirable characteristics for spectroscopic applications in the near IR [1] that the dye laser has in the visible. The tuning range of an individual color center crystal is typically several hundred nanometers, and single-frequency operation with a free running linewidth of much less than 1 MHz can be achieved. CW output powers are on the order of 50 mW. Other presently available sources of tunable IR radiation either have considerably less output power (diode lasers [2], CW difference frequency generation [3]) or operate in a pulsed mode with broad linewidths (parametric oscillators [4], Raman sources).

In this paper we report the operation of a computer controlled CW color center laser spectrometer. With such a spectrometer, it is possible to observe Doppler limited absorptions using standard techniques, or to employ nonlinear spectroscopic techniques to observe extremely high resolution spectra.

## EXPERIMENT ARRANGEMENT

The CCL is depicted schematically in Fig. 1. It consists of a krypton ion pump laser, the color center laser, and diagnostic instrumentation. Details of the color center laser design, which utilizes an astigmatically compensated, collinearly pumped three mirror cavity [1], are described in [5]. The laser is

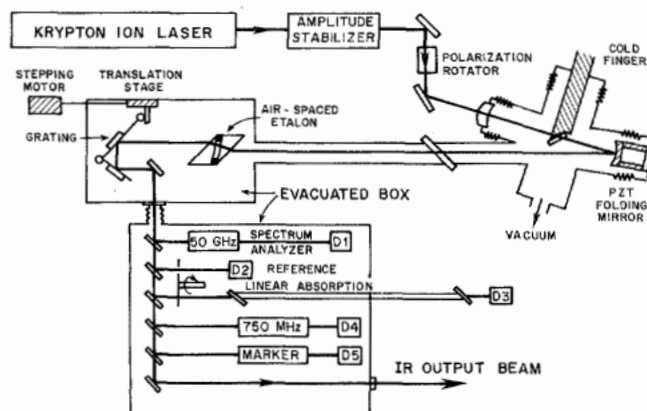


Fig. 1. Schematic for computer controlled CW color center laser spectrometer.

tuned by appropriate adjustment of three elements: a Littrow mounted diffraction grating, an air-spaced etalon, and a PZT mounted folding mirror. The grating functions both as a tuning element and output coupler [6]. The zeroth-order reflection couples 20 percent of the power out of the cavity.

With the etalon removed from the cavity, the laser operates in two longitudinal modes which are separated in frequency by 4.17 GHz. This two-mode operation results from the spatial hole burning effect in the standing wave cavity [7]. Coarse resolution survey scans can be made in this configuration for rapid mapping of a spectrum. Insertion of an air spaced etalon [8] with free spectral range (FSR) of 25.3 GHz and 30 percent reflective coating gives stable single-mode operation with a linewidth of less than 1 MHz [7]. Scanning only the etalon, the laser can be tuned in cavity mode steps of 250 MHz over a range of about 20 GHz. To achieve continuous narrow-line tuning, the cavity length must be adjusted by concurrently tracking the folding mirror.

Due to the strength of many atmospheric absorption lines in this wavelength region, it is necessary to evacuate the entire tuning arm of the CCL. Even with low pressure (0.5 torr), laser tuning is often affected because of mode competition effects which cause the laser frequency to discontinuously jump over instead of smoothly tuning through an atmospheric absorption line. Evacuation to a pressure of less than 10 mtorr with an absorption pump eliminates such behavior.

In order to monitor single-frequency operation and tuning, portions of the laser output are directed to two spectrum analyzers (FSR = 750 MHz and 60 GHz) and a stable marker cavity (FSR = 500 MHz). Strong variations in the finesse of these instruments by atmospheric absorption lines are pre-

Manuscript received February 19, 1980; revised June 23, 1980. This work was supported by the Department of Energy, the National Science Foundation, and the Robert A. Welch Foundation.

G. Litfin is with the Institut für Angewandte Physik, Universität Hannover, D3000 Hannover, Germany.

C. R. Pollock and F. K. Tittel are with the Department of Electrical Engineering, Rice University, Houston, TX 77001.

J. V. V. Kasper is with the Department of Chemistry, University of California, Los Angeles, CA 90024.

R. F. Curl, Jr. is with the Department of Chemistry, Rice University, Houston, TX 77001.

vented by placing them in another evacuated box. For wavelength calibration, a 60 cm sample cell containing a gas with a well-known spectrum and a reference detector monitoring the laser power are used. All IR signals are observed with lead sulfide detectors covered by germanium windows. The remaining output power (60 percent) is available for the experiment.

The spectrometer is interfaced to a Digital Equipment Corporation (DEC) LSI-11 minicomputer using various CAMAC modules and a Kinetic Systems 3912 controller [9]. The computer tunes the laser in open loop operation by synchronously adjusting the grating angle, etalon separation, and cavity length at the proper rates. A stepping motor, driven by a BiRa 3101 driver, rotates the grating via a sine drive. The position of the motor relative to a fixed limit switch thus determines the grating angle. The air-spaced etalon and PZT mounted mirror are controlled by high voltage amplifiers, which are driven by appropriate voltages from a Kinetic Systems 3112 digital-to-analog converter. Data from the various signals are acquired via a BiRa 4301 analog-to-digital converter. Both 60 Hz line frequency and an SEC RTC-01 real time clock are used for timing of data acquisition and scanning.

#### OPERATION AND PERFORMANCE

The key to precise tuning of the laser is proper concurrent tracking of the tuning elements. Cross-reference tables which correlate grating motor position and etalon voltage with either wavelength or frequency are generated as described below. Scanning is accomplished by incrementing an internal frequency counter at a selected rate and setting the grating and etalon to the positions specified by the tables. The accuracy of subsequent scans is determined by these tables and the reproducibility of these scans by the stability of the laser.

In order to generate the cross-reference tables, each tuning element must be calibrated. With the etalon removed from the cavity, the grating position as a function of wavelength is determined by scanning the laser with a known gas in the sample cell and identifying some of the peaks with precisely known transitions. The software fits these data with a cubic polynomial to incorporate any deviations arising from the sine drive and generates a table over the entire range. This table has an absolute accuracy of better than  $0.5 \text{ cm}^{-1}$ . Recalibration is necessary only if one of the optical elements in the cavity is readjusted. Low resolution scans with a linewidth of  $0.1 \text{ cm}^{-1}$  can now be routinely and accurately made. The upper trace of Fig. 2 shows, as an example, a low-resolution scan of the overtone 2-0 absorption band of NO.

For high-resolution operation, the etalon must be placed back in the cavity. Calibration of the etalon requires accurate determination of its FSR and frequency change per volt characteristics. The FSR is found by scanning the grating with the etalon held at a fixed voltage. As the grating sweeps through successive transmission peaks of the etalon, the output power is modulated in a sinusoidal fashion. Autocorrelation of this signal by the computer accurately determines the change in grating position and hence the frequency spacing which corresponds to one FSR of the etalon. The frequency versus voltage response is determined by scanning only the etalon and

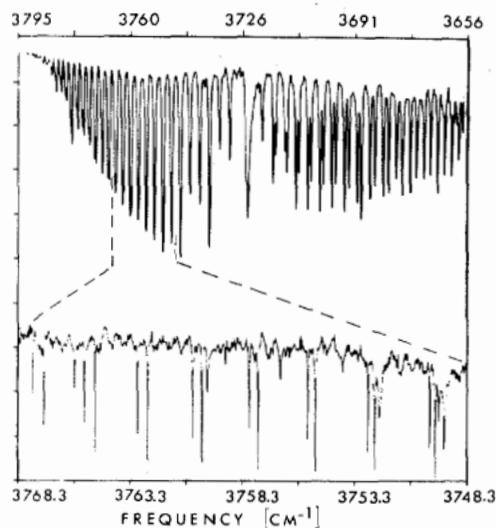


Fig. 2. Absorption spectrum of the 2-0 overtone of NO at  $2.68 \mu\text{m}$ . Upper trace: low resolution scan using only the grating as tuning element taken with a pressure of 500 torr. Lower trace: scan with cavity mode resolution at 40 torr NO pressure. The  $R(27/2)$  to  $R(13/2)$  lines are displayed. Additional lines are due to water impurities.

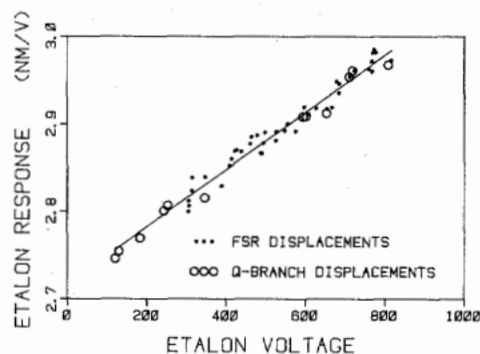


Fig. 3. Dependence of the etalon response on the PZT voltage.

recording either the transmission of a marker cavity or of an absorption spectrum.

Open loop operation of the air spaced etalon requires consideration of its wavelength dependence and the nonlinearities of the high voltage amplifier and PZT. The wavelength dependence (scanning 1 FSR corresponds to increasing the spacing by  $\lambda/2$ ) causes a linear increase of the required scanning distance with wavelength. The nonlinear response of the amplifier and PZT leads to the need to express etalon spacing as a nonlinear (quadratic) function of voltage. These effects must be included in developing the cross-reference table.

The variation of the etalon response as a function of the applied voltage is shown in Fig. 3. The etalon response  $\alpha$  is defined by

$$\alpha = \frac{\Delta l}{V_2 - V_1}$$

where  $\Delta l$  is the expansion of the etalon which occurs by increasing the voltage from  $V_1$  to  $V_2$ . The abscissa in Fig. 3 is simply the average of the two voltages. The data represented by circles are values for the etalon response derived from three separate scans over the Q-branch of NO. These values were determined using known frequency separations of adjacent

$Q$ -branch transitions [10], the corresponding difference in etalon voltage, and the FSR of the etalon, which is measured with the previously described autocorrelation technique. Those data marked with dots are values for the etalon response obtained from analysis of repeated features in scans over several FSR using 35 different NO absorptions spanning the spectral range of the CCL. They were easily determined because the change in spacing is one-half of a wavelength. A single straight line fits all data with a standard deviation of 0.010 nm/V, implying an accurate quadratic relationship between etalon frequency and voltage. The use of a quadratic relationship results in a frequency error of at most 250 MHz (corresponding to one cavity mode) over a scan interval of 3000 GHz.

Long range single-mode scans can be made by scanning both the etalon and the grating. The computer automatically sets the etalon back after it has scanned one FSR, followed by a suitable delay (typically 2 s) to allow transient ringing and drift to decay before resumption of scanning. In this manner, scans of up to  $100\text{ cm}^{-1}$  have been made with a resolution of 250 MHz ( $0.01\text{ cm}^{-1}$ ) as determined by the cavity mode spacing. The lower trace of Fig. 2 shows a high-resolution scan of a  $20\text{ cm}^{-1}$  segment of the  $R$ -branch of NO. For different rotational quantum numbers, pairs of absorption lines belonging to the  $^2\pi_{1/2}$  and  $^2\pi_{3/2}$  transitions are clearly resolved. Due to impurities in our NO sample, additional lines appear which probably arise from  $\text{H}_2\text{O}$  absorptions.

The cross-reference table for the etalon spacing must be periodically updated (generally each day at start-up) because of drifting of the amplifier and etalon temperature. This proved to be a simple matter of an additive shift of the entries in the table. The magnitude of the shift is that needed for the most stable single-mode operation as observed with the spectrum analyzers. Once the cross referencing is set, long range single-mode scans can be routinely made without further adjustment.

Smooth single-mode scans without cavity mode jumps are made by additionally tracking the cavity length. This is done with the PZT controlled folding mirror which is repetitively scanned and set back by the computer, again with suitable delay for settling. The technique for controlling the cavity length is the same as described above for the etalon.

Fig. 4 shows such a high-resolution scan of the  $R(9/2)$  line of NO. The  $\Lambda$ -doubling of the  $^2\pi_{1/2}$  transition with a separation between the two peaks of 305 MHz [11] is clearly resolved. The resolution of this measurement is limited by the Doppler broadening which is significantly wider than the spectrometer linewidth.

So far the spectrometer can be used in the range from 2.3 to  $3.2\text{ }\mu\text{m}$  with  $F_A(11)$  center crystals (KCl:Li, RbCl:Li) and  $F_B(11)$  center crystals (KCl:Na). The operating regime of the spectrometer should be extendable to the entire tuning range of CW color center lasers from 800 to  $3.3\text{ }\mu\text{m}$  by use of other crystals [12]. This source opens new possibilities for high-resolution, high sensitivity molecular spectroscopy, and laser photochemistry. As a first application of this spectrometer, the detection of low concentrations of free radicals has been demonstrated using magnetic rotation spectroscopy [13].

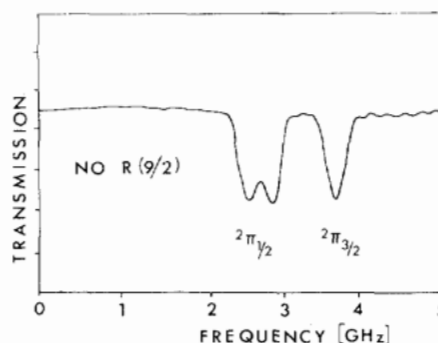


Fig. 4. Continuous single-mode scan over the  $R(9/2)$  transition with 5 torr NO pressure. Both  $^2\pi_{1/2}$  and  $^2\pi_{3/2}$  transitions are observed with the  $^2\pi_{1/2}$  transition split by  $\Lambda$ -doubling. The separation of the  $\Lambda$ -doubling components is 305 MHz.

#### ACKNOWLEDGMENT

The authors would like to thank E. M. Chae for technical assistance.

#### REFERENCES

- [1] L. F. Mollenauer and D. H. Olson, "Broadly tunable lasers using color centers," *J. Appl. Phys.*, vol. 46, pp. 3109-18, 1975; H. Welling, G. Litfin, and R. Beigang, "Tunable infrared lasers using color centers," in *Laser Spectroscopy III*, J. L. Hall and J. L. Carlsten, Eds. Berlin: Springer-Verlag, 1977, pp. 370-375.
- [2] E. D. Hinkley, K. W. Nill, and F. A. Blum, "Infrared spectroscopy with tunable lasers," in *Laser Spectroscopy of Atoms and Molecules*, H. Walther, Ed. Berlin: Springer-Verlag, 1976, pp. 127-196.
- [3] A. S. Pine, "IR spectroscopy via difference-frequency generation," in *Laser Spectroscopy III*, J. L. Hall and J. L. Carlsten, Eds. Berlin: Springer-Verlag, 1977, pp. 376-381.
- [4] R. L. Byer, "Parametric oscillators," in *Tunable Lasers and Applications*, A. Mooradian, T. Jaeger, and P. Stokseth, Eds. Berlin: Springer-Verlag, 1976, pp. 70-80.
- [5] G. Litfin and R. Beigang, "Design of tunable cw color center lasers," *J. Phys. E: Sci. Instrum.*, vol. 11, pp. 984-986, 1978.
- [6] K. German, "Diffraction grating tuners for cw lasers," *Appl. Opt.*, vol. 18, pp. 2348-2349, 1979.
- [7] R. Beigang, G. Litfin, and H. Welling, "Frequency behaviour and linewidth of cw single mode color center lasers," *Opt. Commun.*, vol. 22, pp. 269-271, 1977.
- [8] Burleigh FCL - 500.
- [9] C. R. Pollock, J. V. V. Kasper, G. K. Ernst, W. E. Ernst, S. Blit and F. K. Tittel, "Computer controlled cw laser spectrometer," *Appl. Opt.*, vol. 18, pp. 1907-1912, 1979.
- [10] K. E. J. Hallin, J. W. C. Johns, D. W. Leppard, A. W. Mantz, D. L. Wall, and K. Narahari Rao, "The infrared emission spectrum of  $^{14}\text{N}^{16}\text{O}$  in the overtone region and determination of Dunham coefficients for the ground state," *J. Molec. Spectrosc.*, vol. 74, pp. 26-42, 1979; A. Henry, M. F. Le Moal, P. Cardinet, and A. Valentin, "Overtone bands of  $^{14}\text{N}^{16}\text{O}$  and determination of molecular constants," *J. Molec. Spectrosc.*, vol. 70, pp. 18-26, 1978.
- [11] A. S. Pine, J. W. C. Johns, and A. G. Robiette, " $\Lambda$ -doubling in the  $v=2-0$  overtone band in the infrared spectrum of NO," *J. Molec. Spectrosc.*, vol. 74, pp. 52-69, 1979.
- [12] Lasers using  $F_2^+$  (and  $F_2^+$  like) center crystals presently operate from 800 nm to  $2.5\text{ }\mu\text{m}$  with the sole exception of the range 1.9-2.0  $\mu\text{m}$ . It is expected this gap will be filled in the near future. See, for example, L. F. Mollenauer, "Dye-like lasers for the 0.9-2  $\mu\text{m}$  region using  $F_2^+$  centers in alkali halides," *Opt. Lett.*, vol. 1, pp. 164-5, 1977; L. F. Mollenauer and D. M. Bloom, "Color-center laser generates picosecond pulses and several watts cw over the 1.24-1.45  $\mu\text{m}$  range," *Opt. Lett.*, vol. 4, pp. 247-249, 1979; W. Gellermann, F. Luty, K. Koch, and G. Litfin, " $F_2^+$  center stabilization and tunable laser operation in  $\text{OH}^-$  doped alkali halides," *Phys. Stat. Solidi*, vol. 57, pp. 411-18, 1980; I. Schneider and M. J. Marrone, "Continuous-wave laser action of  $[F_2^+]_A$  centers in sodium-doped KCl crystals," *Opt. Lett.*, vol. 4, pp. 390-392, 1979; I. Schneider and C. L. Marquardt, "Tunable, con-

tinuous-wave laser action using  $[F_2^+]_A$  centers in lithium-doped  $KCl_2$ ," *Opt. Lett.*, vol. 5, pp. 214-215, 1980.

- [13] G. Litfin, C. R. Pollock, R. F. Curl, Jr., and F. K. Tittel, "Sensitivity enhancement of laser absorption spectroscopy by magnetic rotation effect," *J. Chem. Phys.*, June 15, 1980.

G. Litfin, photograph and biography not available at the time of publication.

C. R. Pollock, photograph and biography not available at the time of publication.

J. V. V. Kasper, photograph and biography not available at the time of publication.

R. F. Curl, Jr., photograph and biography not available at the time of publication.

Frank K. Tittel (SM'72), for a photograph and biography, see page 948 of the September 1980 issue of this JOURNAL.

## Comparison of Experimental and Theoretical Excited-State Spectra for Rhodamine 6G

PETER R. HAMMOND

**Abstract**—The stimulated emission cross section ( $\sigma_e$ ) and the excited-state absorption cross section ( $\sigma^*$ ) for this dye are resolved across the fluorescence and the lowest energy ground-state absorption bands. The absorption is weak ( $\sim 0.4 \times 10^{16} \text{ cm}^2$ ), particularly at the longer wavelengths [Fig. 3(c)]. Lasing properties are predicted from Fig. 4(b), which shows a plot of the ( $\sigma_e$ ) curve displaced with respect to the  $S_1$  state as the zero-energy level of reference, on top of the long-axis polarized ground-state absorption band. Spectral assignments are proposed in terms of symmetry arguments based on this observation.

THE understanding and modeling of the physical and chemical behavior of laser dyes requires accurate determination of fluorescence parameters. Previous measurements were reported on the excited-state spectrum of rhodamine 6G [1] and on the decay time and quantum yield [2]. This article calculates the stimulated emission cross section ( $\sigma_e$ ) in an attempt to resolve the excited-state absorption cross section ( $\sigma^*$ ) across the fluorescence and lowest energy ground-state absorption band.

Fig. 1 shows spectra of the ground-state  $S_0(S_n \leftarrow S_0, \text{ where } n = 1, 2 \dots)$  and an experimental curve fitted to point measurements for the lowest excited singlet state  $S_1(S_n \leftarrow S_1, \text{ where } n = 0, 2, 3 \dots)$ . The ground-state cross section ( $\sigma_0$ ) is determined simply from the ratio of the incident ( $I_I$ ) and emerging ( $I$ ) monochromatic beams on a dye sample in conventional equipment, such as a Cary spectrophotometer, according to

$$\ln \frac{I}{I_I} = -N d \sigma_0 \quad (1)$$

where  $N$  is the dye concentration (molecules/c.c.) and  $d$  is the cell path length. If the dye molecules are now converted entirely to the  $S_1$  state, the induced spectrum, if it could be so recorded, would be as shown. At shorter wavelengths there would again be absorption, whereas for wavelengths in the yellow and red the signal would come through amplified. Because rhodamine 6G is a laser dye, the spectrum shows a crossover point from absorption to gain and for the gain region ( $\sigma_e - \sigma^*$ ) is positive. It is this *effective* stimulated emission cross section that is the basic parameter defining lasing behavior. It is related, just as for  $\sigma_0$ , by

$$\ln \frac{I}{I_I} = N d (\sigma_e - \sigma^*). \quad (2)$$

Determination of the  $S_1$  spectrum must be under small-signal conditions, so that there is no distortion of level population, just as it must be for the ground-state spectrum.

The pertinent energy scheme is the customary one shown in Fig. 2. Molecules excited from the lower levels of the  $S_0$  state fall promptly to the lower levels of  $S_1$ . Excitation from here occurs to higher states within the singlet manifold and the system very rapidly returns to  $S_1$  via internal conversion and vibrational relaxation. Loss from  $S_1$  takes place by stimulated and spontaneous emission, by internal conversion back to  $S_0$ , and by intersystem crossing to the triplet. Like the  $S_0$  absorption, the excited singlet absorption is a continuous band spectrum and because the spacing between energy states diminishes at higher energy as the ionization continuum is

Manuscript received January 22, 1980. This work was performed under the auspices of the U.S. Department of Energy under Contract W-7405-Eng-48.

The author is with the Lawrence Livermore Laboratory, Livermore, CA 94550.